



Optics Letters

Beyond the 2D limit: étendue-squeezing line-focus solar concentrators

HÅKON J. D. JOHNSEN,^{1,*}  ASTRID AKSNES,² AND JAN TORGENSEN¹

¹Norwegian University of Science and Technology, Department of Mechanical and Industrial Engineering, Richard Birkelands Vei 2b, Trondheim, Norway

²Norwegian University of Science and Technology, Department of Electronic Systems, O.S. Bragstads plass 2b, Trondheim, Norway

*Corresponding author: hakon.j.d.johnsen@ntnu.no

Received 1 September 2020; revised 15 November 2020; accepted 17 November 2020; posted 17 November 2020 (Doc. ID 406280); published 21 December 2020

Line-focus solar concentrators are commonly designed by extruding a two-dimensional concentrator in the third dimension. For concentration in air, these concentrators are, by the nature of their design, limited by the two-dimensional solar concentration limit of $212\times$. This limit is orders of magnitude lower than the $45000\times$ concentration limit for three-dimensional solar concentrators. Through the use of étendue squeezing, we conceptually show that it is possible to design line-focus solar concentrators beyond this 2D limit. This allows a concentrator to benefit from a line focus suitable for heat extraction through a tubular receiver, while reaching concentration ratios and acceptance angles previously unseen for line-focus concentrators. We show two design examples, achieving simulated $75\times$ concentration and $218\times$ concentration ratios, with a $\pm 1^\circ$ acceptance angle. For comparison, the 2D concentration limit is $57\times$ at this acceptance angle. Étendue-squeezing line-focus solar concentrators, combined with recent developments in tracking integration, may enable the development of a new class of concentrated solar power systems. © 2020 Optical Society of America under the terms of the [OSA Open Access Publishing Agreement](https://doi.org/10.1364/OL.406280)

<https://doi.org/10.1364/OL.406280>

Solar concentrators are essential for efficient utilization of solar thermal energy, and have a fundamental concentration limit in air of

$$C_{\max} = \frac{1}{(\sin \theta_{\max})^2}, \quad (1)$$

where θ_{\max} is the acceptance angle of the concentrator, which must be at least wide enough for the $\theta \approx 0.27^\circ$ divergence half-angle of sunlight. This leads to a solar concentration limit in air of approximately $45000\times$ [1]. To approach the limit, the concentrator must concentrate sunlight in three dimensions, which traditionally means concentrating to a point-like focus. The high fundamental concentration limit enables point-focus solar concentrators to be designed with large acceptance angles and non-ideal optics, and still achieve sufficient concentration for

many applications. In the remainder of this Letter, we will consider the condition $\theta_{\max} = 1^\circ$, where the increased acceptance angle represents an increased tolerance to tracking and surface errors. At this increased acceptance angle, the two-dimensional concentration limit is $3283\times$.

Solar concentrators can also be built to concentrate sunlight to a line focus. Such a line focus is suitable for heat extraction through tubular receivers, and can also be designed to benefit from a simplified one-axis tracking motion. Line-focus concentrators are commonly designed by extruding two-dimensional concentrator geometries, which limits the concentration in air to the 2D concentration limit [1]:

$$C_{\max,2D} = \frac{1}{\sin \theta_{\max}}. \quad (2)$$

For a solar divergence half-angle of $\theta = 0.27^\circ$, the limit is approximately $212\times$, and with the 1° acceptance angle considered in this Letter, it is reduced to $57\times$. The 2D and 3D limits in Eqs. (1) and (2) are plotted against the acceptance angle in Fig. 1.

It has previously been shown that the concentration ratio of linear primary concentrators can be boosted beyond the 2D concentration limit by introducing secondary concentrators close to the line focus, reaching concentration ratios of $300\times$ with one-axis polar tracking [2], or $>1000\times$ with two-axis tracking [3,4]. However, these secondary concentrators achieve their increased concentration ratios by breaking the line focus into a set of small point or line foci, missing the benefit of a true line focus for tubular receivers (as further illustrated in Fig. S3 of Supplement 1). It has also been shown that the 2D limit can be surpassed using nominally linear concentrators where the translational symmetry is broken by ridges in the concentrator, but these have focused on relatively large acceptance angles suitable for stationary solar concentration [5–7].

We show that the common approach of extruding a two-dimensional concentrator is not the only way to design a line-focus concentrator, and demonstrate a method to directly construct a 3D concentrator that concentrates to a line focus. Thus, it is possible to benefit from the high concentration of 3D concentrators while maintaining the practical benefits for heat extraction through tubular receivers placed along a line focus. The use of such a high-concentration line-focus concentrator

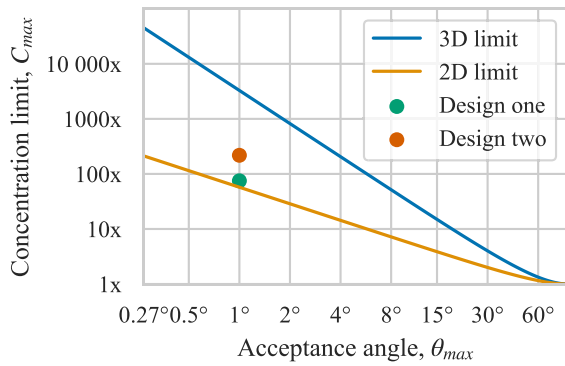


Fig. 1. Concentration limits versus acceptance angle, as given by Eqs. (1) and (2), shown on a log–log scale. The line-focus concentrators demonstrated in this work, represented by the symbols green and red circle, have concentration ratios beyond the 2D concentration limit.

would require two-axis tracking, but this does not necessarily mean that it needs to be mounted on a two-axis external solar tracker. Instead, tracking across the secondary axis may be implemented without physical rotation of the concentrator, similar to what has previously been demonstrated with tracking-integrated solar concentrators for concentrator photovoltaics (CPV) applications [8].

An afocal pair of lens surfaces can be used to compress an optical beam in one axis, while expanding it in the other axis, as illustrated in Fig. 2(a). If the ratio of compression and expansion is 1: N , where N is an integer, the lens pairs can be tessellated in such a way that they fill the front and back surfaces of a lens array, as shown in Fig. 2(b) [9]. This is known as an étendue-squeezing lens array, as introduced in José Blen's 2007 thesis [10], and is an example of the more general concept of étendue squeezing [11]. The étendue-squeezing lens array trades angular extent along one axis against angular extent along the other axis by a factor N [9]. It has been demonstrated for applications such as changing the aspect ratio of the collimated beam from an LED source [9].

By adjusting the lens geometry, the étendue-squeezing lens array can be used to create a solar concentrator with a line focus: instead of emitting the collimated beam, as shown in Fig. 2,

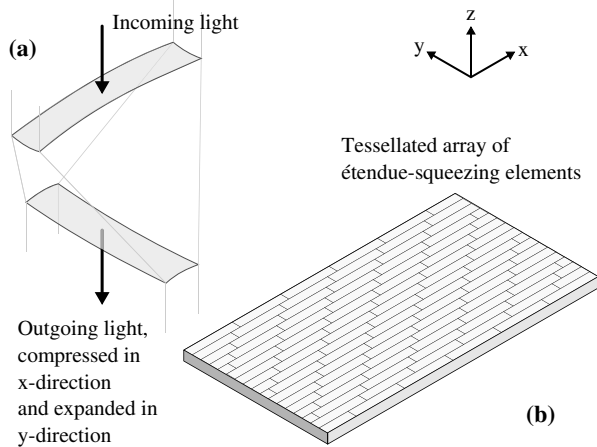


Fig. 2. (a) Principle of étendue squeezing using an afocal lens pair. (b) The lens pairs can be tessellated into a complete étendue-squeezing lens array.

each lens pair can be optimized to redirect the sunlight towards a shared focal line. The principle, as well as a complete solar concentrator, are shown in Fig. 3. Such a concentrator thus becomes a combination of a linear Fresnel lens—redirecting the sunlight towards a shared focal line—and an étendue-squeezing lens array—reducing angular extent in the y direction to permit higher concentration ratios. As shown in the design examples below, this principle enables the concentrator to utilize two-axis tracking and bypass the 2D concentration limit.

To demonstrate the principle, we used numerical optimization to create two line-focus solar concentrators: one concentrator consists of only a double-sided lens array, and the other uses an additional secondary reflector. Both designs were constructed with an étendue squeezing factor of $N = 7$ (the ratio of the short to the long side of the individual rectangular facets is 1:7). The factor seven was chosen as an example, with the aim of being high enough to allow for a significant concentration boost, while low enough to allow for practical implementation. Each individual lens pair was numerically optimized according to its position in the concentrator, using a custom Python ray-tracer. Optimization was performed using a memetic optimization algorithm combining the sequential least squares programming (SLSQP) and differential evolution algorithms from the SciPy library [12]. The optimization was performed in two stages. In the first stage, a small subset of the lens pairs was optimized to identify a realistic geometric concentration ratio where efficiency on the order of 80% could be expected. In the second stage, all lens pairs were independently optimized for maximum efficiency at the geometric concentration ratio chosen from the first stage. The freeform front and back surfaces were represented as sixth-order Legendre polynomials, chosen for being orthogonal in sag on the rectangular lens aperture [13]. Due to the problem's symmetry, only Legendre terms symmetric in the x direction were allowed to be non-zero during optimization. After optimization, the lens pairs were tessellated and combined into a Zemax OpticStudio model to verify and evaluate the complete system. These Zemax OpticStudio models are available in Supplement 1 as we show in Code 1, Ref. [14]. The lens arrays are assumed to be made from PMMA, and illuminated using the AM1.5D spectrum

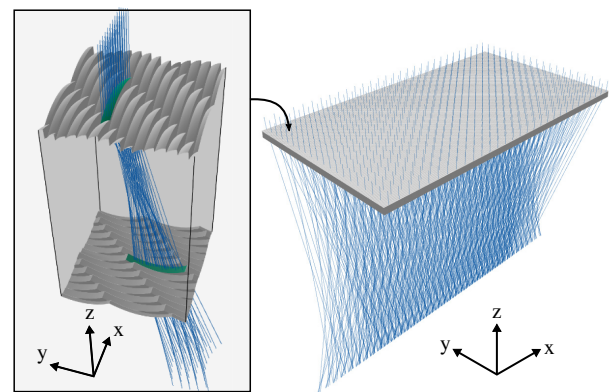


Fig. 3. Solar concentrator utilizing étendue squeezing, consisting of an array of tessellated étendue-squeezing lens pairs. Each lens pair squeezes the beam in the x direction and expands it in the y direction, while redirecting the sunlight towards the common focal line. The cutout shows one such lens pair highlighted in green, and demonstrates how the lens pairs are tessellated into a complete double-sided lens array.

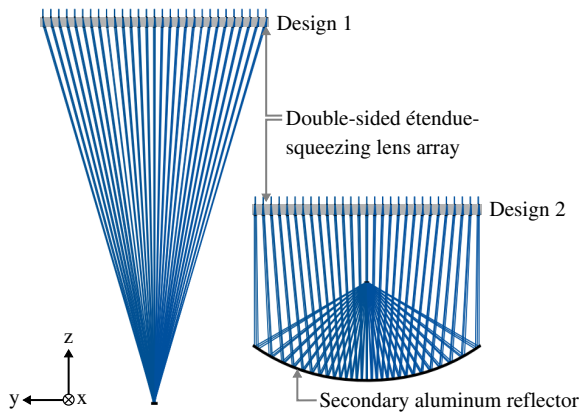


Fig. 4. Ray-traced drawing of the two design examples. Only a subset of the lens pairs is drawn and traced, to reduce clutter in the drawing. In reality, the lens pairs are tessellated to fill the entire front and back surfaces of the lens array, as shown in Fig. 3.

and a top-hat $\pm 1^\circ$ angular distribution. This angular distribution was chosen as an example to demonstrate the possibility of designing for high tolerance to tracking errors. Reflection losses and chromatic aberration were taken into account. For simplicity, volume absorption and surface scattering losses were not included in the simulation of these design examples. For simplicity, the absorbing surface is assumed to be planar. The optimization of concentrator performance with tubular receivers is left for future work, and may involve the adaptation of techniques previously developed for high-concentration 2D concentrators for tubular receivers [15].

The first design example is a double-sided lens array, for operation similar to a linear Fresnel lens. A ray-traced 3D model of the optimized concentrator is shown in Fig. 3, and a 2D drawing is shown in Fig. 4. The concentrator is optimized for a $95\times$ geometric concentration ratio under $\pm 1^\circ$ illumination, and achieves 79.1% efficiency in these conditions. This leads to an effective optical concentration of $C_{\text{eff}} = 0.791 \cdot 95 \approx 75.1$. The resulting concentrator has an optimized numerical aperture of $\text{NA} = 0.32$ ($f/1.47$). The intensity across the focal line of the concentrator is shown in Fig. 5, and the angular acceptance is shown in Fig. 6. Further details about the compression of angular extent performed by this concentrator are shown in Fig. S1 of Supplement 1. This concentrator demonstrates that it is possible to surpass the 2D concentration limit, but the concentration ratio of this example design is still only about 31% higher than the 2D limit. The low numerical aperture of the resulting concentrator indicates that the concentration can be increased by a high numerical aperture secondary concentrator, leading us to the next design example.

The second design example combines the étendue-squeezing lens array with a reflective secondary concentrator assumed to be made from aluminum. The geometry of this reflective secondary concentrator is designed so that the resulting concentrator is approximately aplanatic, a condition that has previously been shown to generate concentrators with performance very close to the fundamental concentration limit [16,17]. The numerical aperture of the resulting concentrator was $\text{NA} = 0.89$, chosen to be relatively close to one for high concentration, while having a more practical geometry than a concentrator fully reaching $\text{NA} = 1$. Optimized for a geometric concentration ratio of

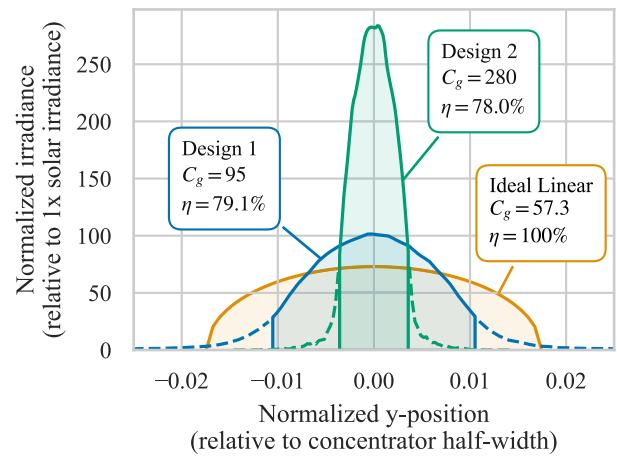


Fig. 5. Intensity profile across the focal line for the two concentrators, under 1 sun AM1.5D illumination with a $\pm 1^\circ$ top-hat angular distribution. The solid lines represent the intensity within the selected geometric concentration ratios. The non-uniform intensity profile of the ideal linear concentrator is caused by the circular $\pm 1^\circ$ angular distribution of the illumination, as further discussed in Supplement 1.

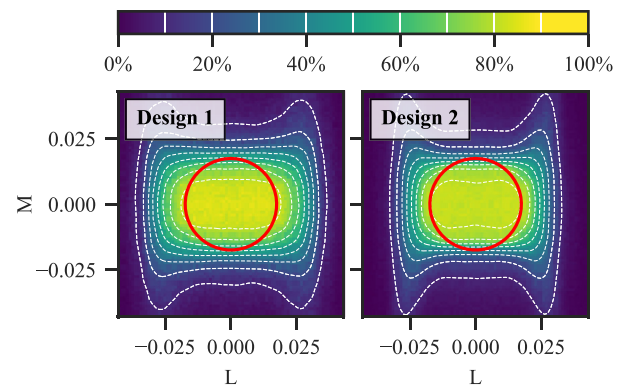


Fig. 6. Optical efficiency of the concentrators as a function of incidence angle, shown as contour plots in direction cosine space. L and M are direction cosines along the x and y axes, respectively. The concentrators are optimized for maximum efficiency under a $\pm 1^\circ$ top-hat angular distribution, which is illustrated by the red circles.

$280\times$, this concentrator achieves 78.0% efficiency under $\pm 1^\circ$ illumination. This leads to an effective optical concentration of $C_{\text{eff}} = 0.780 \cdot 280 \approx 218$. The intensity across the focal line of the concentrator is shown in Fig. 5, and the angular acceptance of the concentrator is shown in Fig. 6.

The presented design examples have modeled efficiencies of 79.1% and 78.0%, respectively. The losses arise from reflection losses in the lens array, geometric losses from shading of neighboring elements in the lens array, absorption losses in the reflector, and finally, a non-unity intercept factor. Volume absorption losses, surface scattering losses, and losses due to manufacturing tolerances were not included in these simulations. The relative magnitude of each loss was measured by selectively disabling loss mechanisms while simulating the system, and are summarized in Table 1.

A consequence of the decreased angular extent along the y axis in these concentrators is an increased angular extent along

Table 1. Relative Magnitude of Different Losses in the Designs

	Design 1	Design 2
Lens array reflection loss	7.8%	7.6%
Lens array geometric loss	3.2%	2.6%
Reflector absorption loss	—	5.4%
Intercept loss	11.4%	8.3%
Complete efficiency	79.1%	78.0%

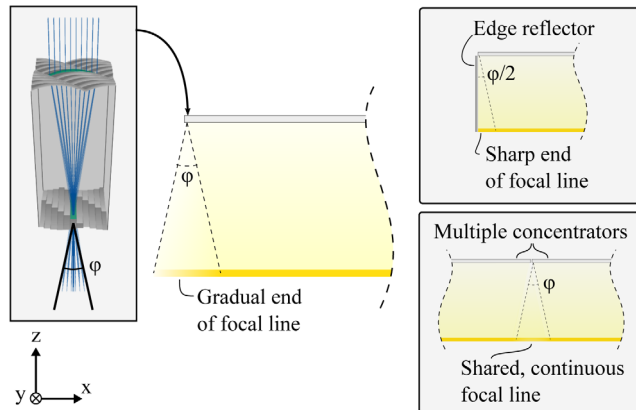


Fig. 7. Étendue-squeezing lens pairs increase the angular extent of the light along the x direction, which introduces a softening at the ends of the focal line. This effect can be circumvented by creating a long assembly of concentrators sharing the same focal line, or by using an edge reflector.

the x axis. This angular extent leads to a gradual reduction in intensity at the ends of the line focus, as illustrated in Fig. 7. The effect can be eliminated by using edge reflectors, or the concentrator modules can be placed in long enough solar collector assemblies that such edge effects become negligible—similar to how conventional parabolic trough solar concentrators are organized in long solar collector assemblies.

Both of the presented design examples demonstrate the possibility of utilizing étendue squeezing to go beyond the 2D concentration limit, as plotted in Fig. 1. This may represent a new class of solar concentrators, achieving the high concentration and high acceptance angle of three-dimensional concentrators, while maintaining the linear and modular geometry of line-focus solar concentrators. The combination of such concentrators with tracking integration to achieve the required two-axis solar tracking without needing to rotate the concentrator across two axes will be of interest for future research. One potential approach for such tracking integration is beam-steering lens arrays [18], which can perform one- (or two-) axis tracking using millimeter-scale lateral translation and emit collimated sunlight for concentration by an étendue-squeezing concentrator. The presented design examples are chosen to demonstrate the concentration abilities of étendue-squeezing solar concentrators. Still, they are not necessarily the most economical and practical way to implement an étendue-squeezing concentrator. Further research is needed to identify designs that show a good trade-off among efficiency, concentration, and manufacturability.

In summary, we have shown through two design examples how étendue squeezing can be used to design line-focus concentrators not limited by the 2D concentration limit. To the best of our knowledge, this type of concentrator has not previously been reported in the literature, and the possibility of such concentrators has not previously been appreciated. We have further proposed how developments in tracking integration can be used to circumvent the need for two-axis tracking of these concentrators. If a manufacturable and practical étendue-squeezing solar concentrator can be combined with tracking integration, this may constitute a promising path towards a new class of concentrated solar power, combining the high concentration of heliostats with the modular nature of parabolic trough concentrators.

Acknowledgment. Portions of this work were presented at the *SPIE Optical Engineering + Applications* conference in 2020, paper number 1149509 [19].

Disclosures. The authors declare no conflicts of interest.

See [Supplement 1](#) for supporting content.

REFERENCES

- R. Winston, J. C. Minano, P. G. Benitez, N. Shatz, and J. C. Bortz, *Nonimaging Optics* (Elsevier Science, 2005).
- M. Brunotte, A. Goetzberger, and U. Blieske, *Sol. Energy* **56**, 285 (1996).
- T. Cooper, G. Ambrosetti, A. Pedretti, and A. Steinfeld, *Appl. Opt.* **52**, 8586 (2013).
- B. Wheelwright, R. Angel, and B. Coughenour, in *Classical Optics* (Optical Society of America, 2014), paper ITh1A.2.
- M. Rönnelid and B. Karlsson, *Appl. Opt.* **37**, 5222 (1998).
- J. C. Bortz, N. E. Shatz, and R. Winston, *Proc. SPIE* **4446**, 201 (2001).
- J. Nilsson, R. Leutz, and B. Karlsson, *Sol. Energy Mater. Sol. Cells* **91**, 525 (2007).
- H. Apostoleris, M. Stefancich, and M. Chiesa, *Nat. Energy* **1**, 16018 (2016).
- P. Benitez, J. C. Miñano, and J. Blen, in *Illumination Engineering* (Wiley, 2013), pp. 71–99.
- J. Blen, “Design of multiple free-form optical surfaces in three dimensions,” Ph.D. thesis (Universidad Politécnica de Madrid, 2007).
- P. Benitez, J. C. Miñano, J. Blen, O. Dross, and F. García, in *International Nonimaging Optics Workshop* (2005), pp. 13014–13020.
- E. Jones, T. Oliphant, and P. Peterson, “SciPy: open source scientific tools for Python,” 2001, <http://www.scipy.org/>.
- M. I. Nikolic, P. Benitez, B. A. Narasimhan, D. Grabovickic, J. Liu, and J. C. Miñano, *Opt. Eng.* **55**, 071204 (2016).
- H. J. D. Johnsen, A. Aksnes, and J. Torgersen, “Zemax OpticStudio models of étendue-squeezing solar concentrators,” figshare (2020) <https://doi.org/10.6084/m9.figshare.12894809>.
- P. Benitez, R. García, and J. C. Miñano, *Appl. Opt.* **36**, 7119 (1997).
- J. M. Gordon, *Opt. Express* **18**, A41 (2010).
- E. T. A. Gomes, N. Fraidenraich, O. C. Vilela, C. A. A. Oliveira, and J. M. Gordon, *Sol. Energy* **191**, 697 (2019).
- H. J. D. Johnsen, A. Aksnes, and J. Torgersen, *Opt. Express* **28**, 20503 (2020).
- H. J. D. Johnsen, A. Aksnes, and J. Torgersen, *Proc. SPIE* **11495**, 1149509 (2020).